LA-UR-86-2745

SEP 0 8 1986

CONF-860703--32

Los Alamos National Laboratory is operated by the University of California for the United States Department of Energy under contract W-7405-ENG-36

LA-UR--86-2745

DE86 015342

TITLE: DESIGN, TESTING AND MODELING OF A HIGH-GAIN MAGNETIC FLUX-COMPRESSION GENERATOR

AUTHOR(S): M. G. Sheppard, X-10, B. L. Freeman, M-6, R. L. Bowers, X-10
J. H. Brownell, X-10, C. M. Fowler, M-6, J. N. Fritz, M-6,
A. E. Greene, X-10, S. P. Marsh, M-6, T. A. Oliphant, X-10,
D. L. Tubbs, X-2 and D. L. Weiss, X-10

SUBMITTED TO: Megagauss Magnetic Field Generation and Related Topics, Santa Fe, NM, July 14-17, 1986

DISCLAIMER

MASTER

Los Alamos Los Alamos National Laboratory
Los Alamos, New Mexico 87545

DESIGN, TESTING, AND MODELING OF A HIGH-GAIN MAGNETIC FLUX-COMPRESSION GENERATOR*

M. G. Sheppard, B. L. Freeman, R. L. Bowers, J. H. Brownell,
C. M. Fowler, J. N. Fritz, A. E. Greene, S. P. Marsh, T. A. Oliphant,
D. L. Tubbs, and D. L. Weiss

Los Alamos National Laboratory
P.O. Box 1663
Los Alamos, New Mexico 87545 USA

ABSTRACT

Using a simultaneously initiated cylindrical explosive, a coaxial magnetic flux-compression generator (FCG) was designed to test high-current-gain limitations. A coaxial design with a lossless gain of ~100:1 was chosen for its efficiency, relative simplicity, and calculability. Theoretical design included analytic modeling as well as 1-D and 2-D hydrodynamic and MHD calculations. A 69.3-cm cylinder of PBX-9501 high explosive, 20.3 cm in diameter, was used to drive the Al armature into a Cu stator. The initial current supplied by a capacitor bank was ~3 MA which produced a final current ~75 MA. Details of the experiment and a comparison with calculations are presented.

I. INTRODUCTION AND GOALS

Many advances in understanding and performance of magnetic Flux Compression Generators (FCG) have occurred since the concept of using high-explosive (HE) to push a metal conductor and compress a trapped magnetic field was introduced almost 40 years ago.[1-6] Reference 1 gives an excellent time-line of the early history of flux-compression. In an effort to continue this progress, this paper describes a "simple" FCG experiment that (1) nudges the edge of several parameter ranges; (2) is well diagnosed; and (3) provides a stringent test of present and future theories, models and calculations.

In this experiment a fast high-gain coaxial FCG, driven by an on-axis simultaneous line-initiated explosive, is tested. The FCG was loaded with an initial current of ~3 MA, and the thin aluminum armature was expanded to almost three times its initial diameter to produce a large final current.

A coaxial design was chosen because of its calculationally simple geometry which supports only a B_θ magnetic field. The line-initiation package further simplifies the experiment by insuring a quasi-one-dimensional flux compression stage, another boon

*This work was performed under the auspices of the U.S. Department of Energy.

to modeling simplicity. Finally, the good efficiency of coaxial FCG's also supported the design.

II. EXPERIMENT

Figure 1 shows a three-dimensional cutaway diagram of the coaxial FCG. The central cylinder of PBX-9501 HE is 69.3-cm long with a radius of 10.2 cm. The HE is line-detonated on axis. Surrounding the HE is a 1.3-cm thick shock-absorbing layer of $\rho = 0.2\ g/cm^3$ polystyrene. The HE and plastic are held in place by Al tampers. The Al armature, with an inner radius of 11.4 cm is 0.476-cm thick at the feed (left in the figure) end and 0.635-cm thick at the load end. This linear shim phases the flux compression to avoid shorting the load prematurely. The glide planes are brass and are canted 10° to insure good contact with the armature during generator operation. The feed end glide plane is supported by an insulating lexan washer and is separated from the grounded terminal of the input feed by several sheets of mylar. A ring of detonator switches is timed to produce a jet through the mylar and isolate the FCG from the capacitor bank 2 μs before first armature motion.

The stator is made of 1.3 cm thick Cu sheet which was rolled into a 30.5 cm radius cylinder and welded. Total FCG inductance is 132 nH with the load ring accounting for 1.3 nH. This implies a lossless gain of 101.5. The load ring was convoluted to protect the diagnostics from internal sparks and shocks propagating through the 5 $\times\ 10^{-5}$ torr vacuum. The initial current was supplied through 48 coax cables from a 9000 μF capcitor bank at 16.5 kV.

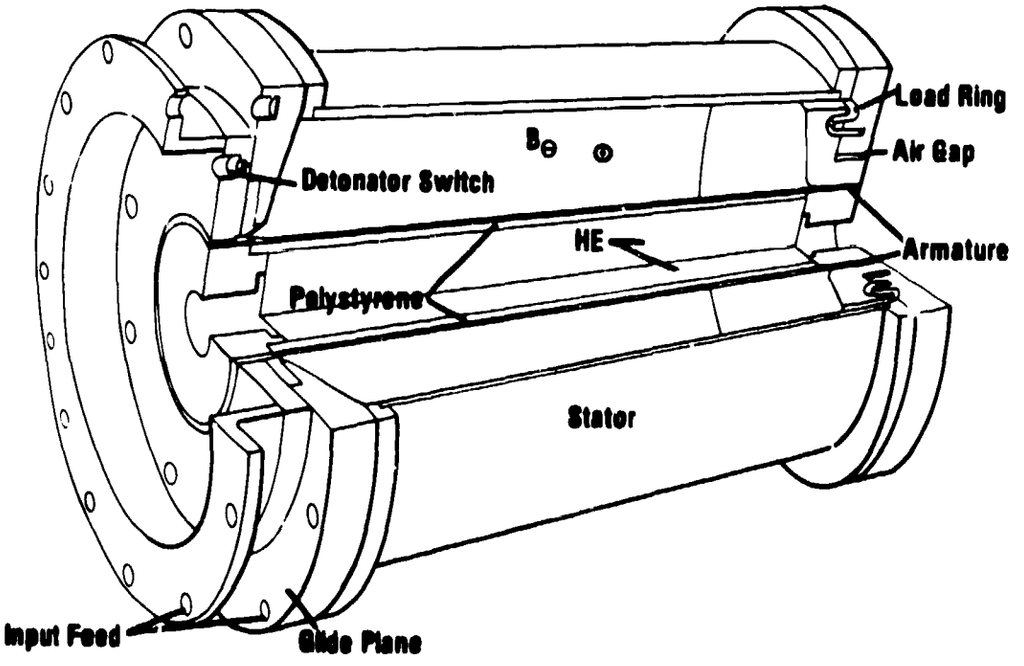

Fig. 1. Coaxial, line-initiated FCG.

III. CALCULATIONS AND MODELING

Results of several different calculations were utilized in the design process. The armature design, including shim angle, thickness and length with relation to the HE cylinder length and positioning of the brass glide planes, was done with a 2-D Eulerian hydrodynamics code. Since the magnetic back pressure was expected to be much less than 25 kbars ($B_{max} \leq 0.8$ MG) for most of the operation time, field effects were ignored during this stage of the design. Results of these simulations are presented in Figs. 2 and 3. The basic armature design was taken from the Mark 101 (see Fowler et al., this issue) and adapted to accommodate the larger diameter required for the plastic shock-absorbing layer and to insure smooth contact with the glide planes during its three-fold expansion. The air gap just below the load ring (Fig. 3) was required to diffuse shocks in the glide plane and protect load ring diagnostics. These calculations were found to be insensitive to inclusion of material strength.

One-dimensional Lagrangian hydrodynamics calculations were done to investigate the effects of different density shock-absorbing layers between the HE and the armature. Figures 4-6 show comparison of calculated pressure profiles and armature interface position and velocity histories for polystyrene densities of 0.2 and 1.04 g/cm.[3] The lower density plastic gives a gentler, more sustained push to the armature, thus keeping the temperature down, the conductivity up, and ultimately the velocity higher.

Armature dynamics were also checked with several 1-D Lagrangian and Eulerian hydrodynamics calculations at different positions along the symmetry axis. Hydrodynamic motion is almost entirely radial (1-D) for this design. Armature interface histories at five locations along the symmetry axis are displayed in Fig. 7. The armature velocity averages about 0.42 cm/μs.

An estimate of magnetic flux loss in the FCG was obtained by calculating a 1-D version (i.e., no armature shim) with a 1-D implicit Lagrangian magnetohydrodynamics (MHD) code. This code includes models for HE detonation and Joule heating, as well as time dependent external circuits to treat the capacitor bank discharge, the closing switch, the inductive load ring, and resistive losses into the glide plane and load ring walls. Losses into the armature and stator walls were calculated within the code using a linear diffusion approximation and resistivity models for Cu and Al as functions of temperature and density. A time dependent resistance for the glide plane and load ring walls was estimated by combining calculated skin depths and resisitivities in the stator with the time dependent current pathlength through the glide plane and load ring walls. This resistance averaged a few times 10^{-5} Ω. These calculations predicted that 38% of the total initial flux would be compressed into the 1.3 nH load at generator burnout. With an initial current of 3 MA, this translates to a final predicted current of 116 MA, or a predicted gain of 38.6.

Since the 1-D calculations cannot account for the armature shim, the predicted inductance history (and therefore current history, I(t)) has too steep of a gradient. To better estimate dI/dt, the quantity actually measured, a circuit model which utilizes an empirical flux loss model, $\phi(t) = \phi_0 exp(-(t/\tau)^2)$, and 2-D geometry input was employed. The quantity τ was fit to the 1-D MHD calculation such that $\phi(t_{burnout})/\phi_0 = 0.38$. This value is consistent with results obtained by Zharinov et al[7] using a similar coaxial, line-initiated FCG. The curves in Fig. 7 provided 2-D geometry input for calculating the FCG inductance history. The results of the circuit simulations are not sensitive to reasonable excursions about the shape of $\phi(t)$ which

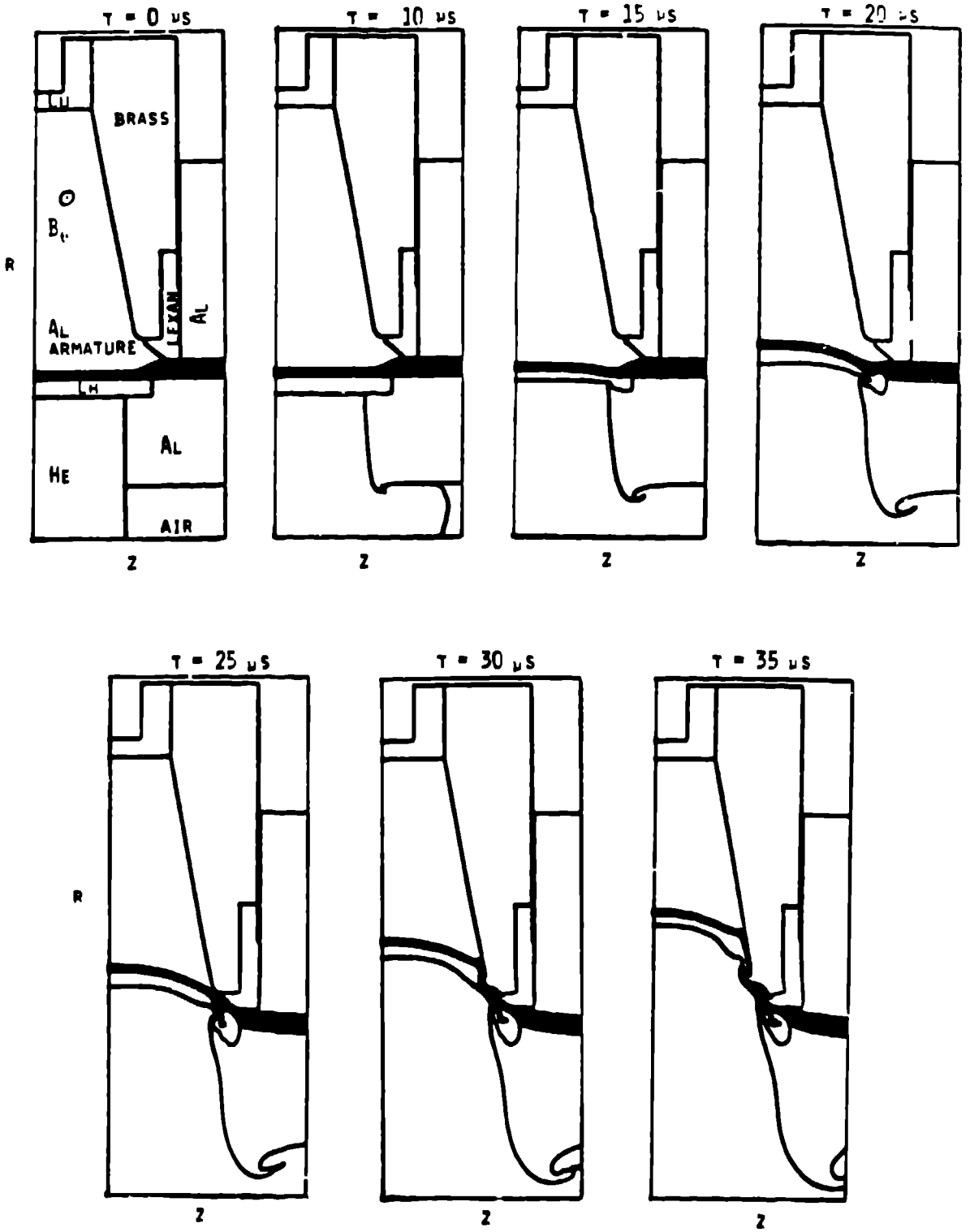

Fig. 2. Time sequences of interfaces for feed end.

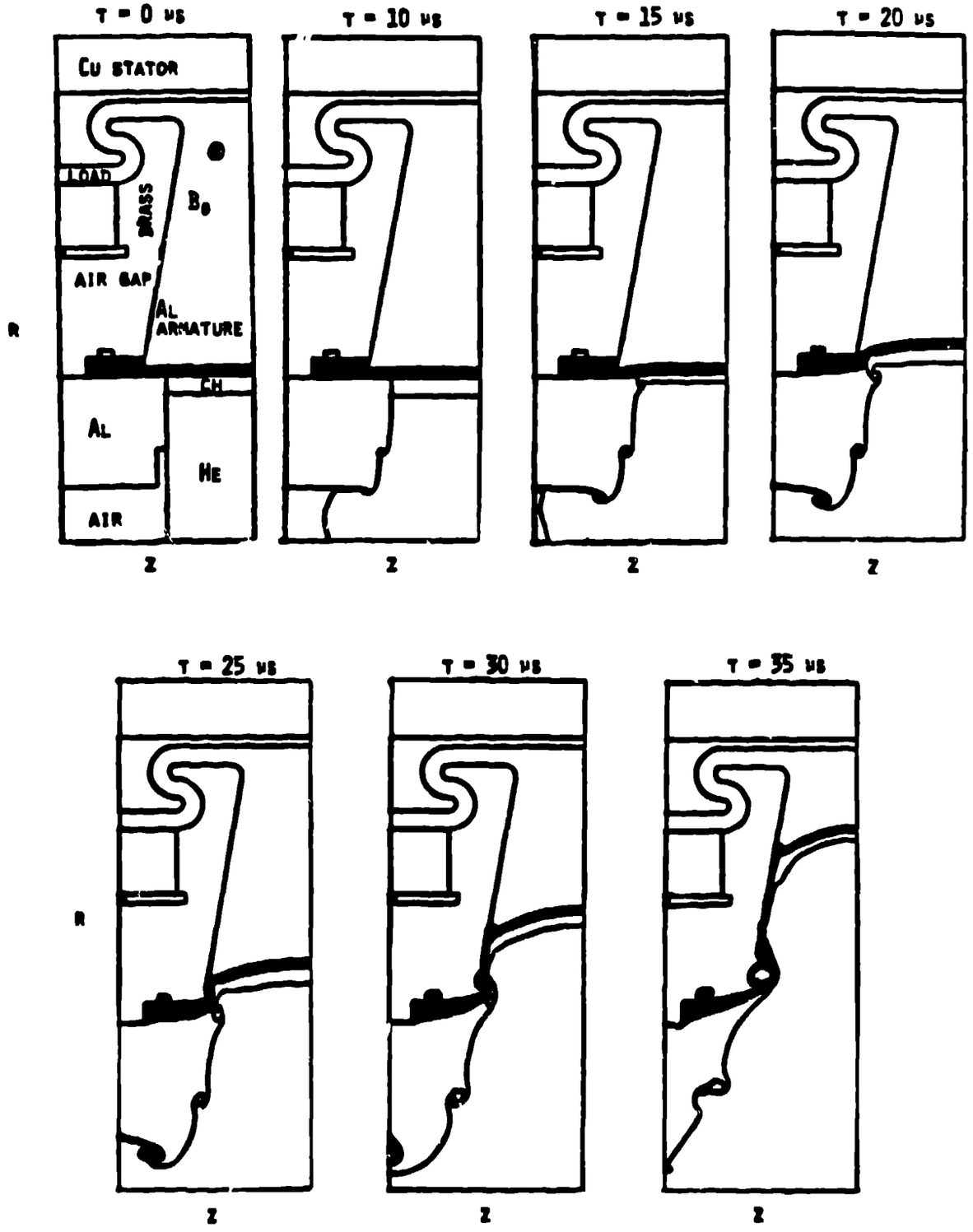

Fig. 3. Time sequences for interfaces of load end.

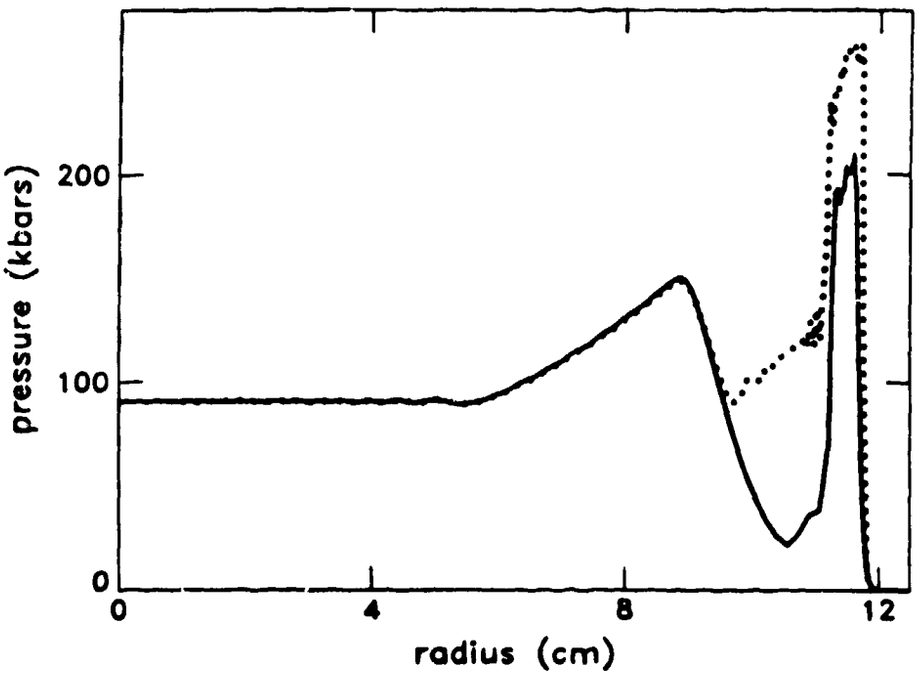

Fig. 4. Comparison of pressure profile in HE, polystyrene $\rho = 0.2g/cm^3$ (solid) and $\rho = 1.04g/cm^3$ (dotted), and Al 1 μs before first motion.

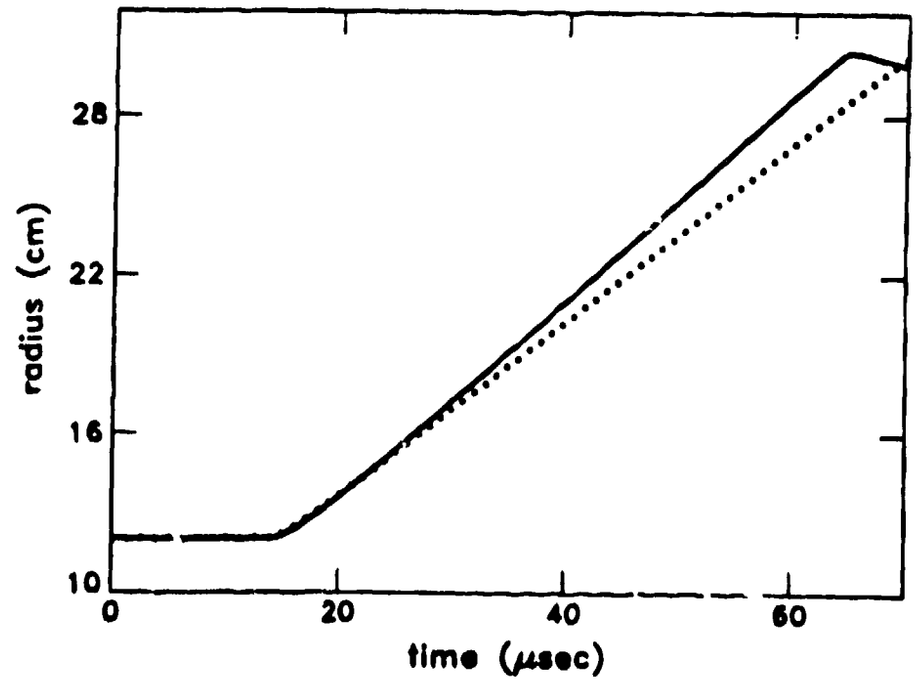

Fig. 5. Comparison of armature interface position with $\rho = 0.2g/cm^3$ (solid) and $\rho = 1.04g/cm^4$ (dotted) polystyrene.

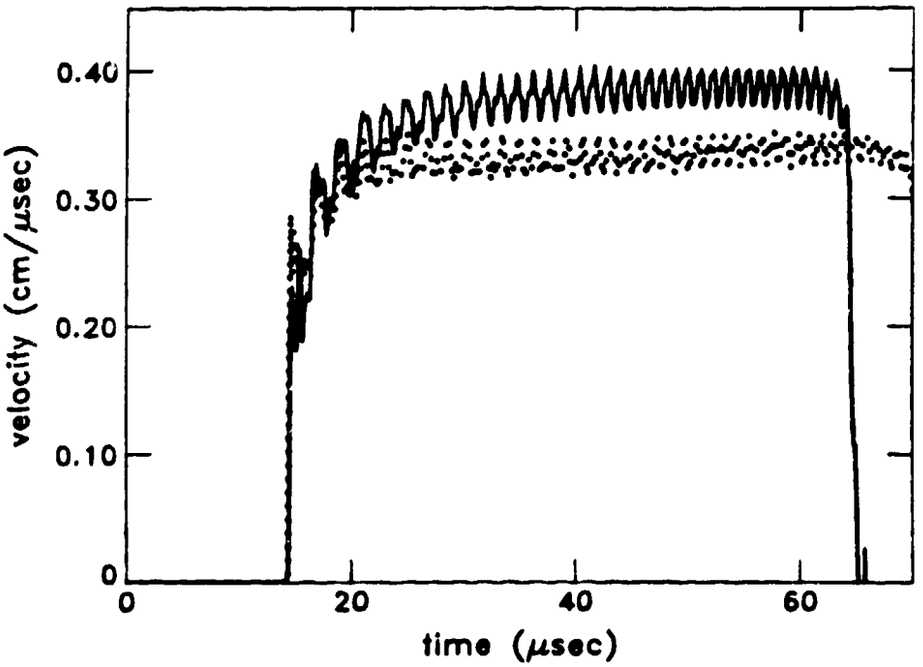

Fig. 6. Comparison of armature velocity with $\rho = 0.2g/cm^3$ and $\rho = 1.04g/cm^3$ polystyrene.

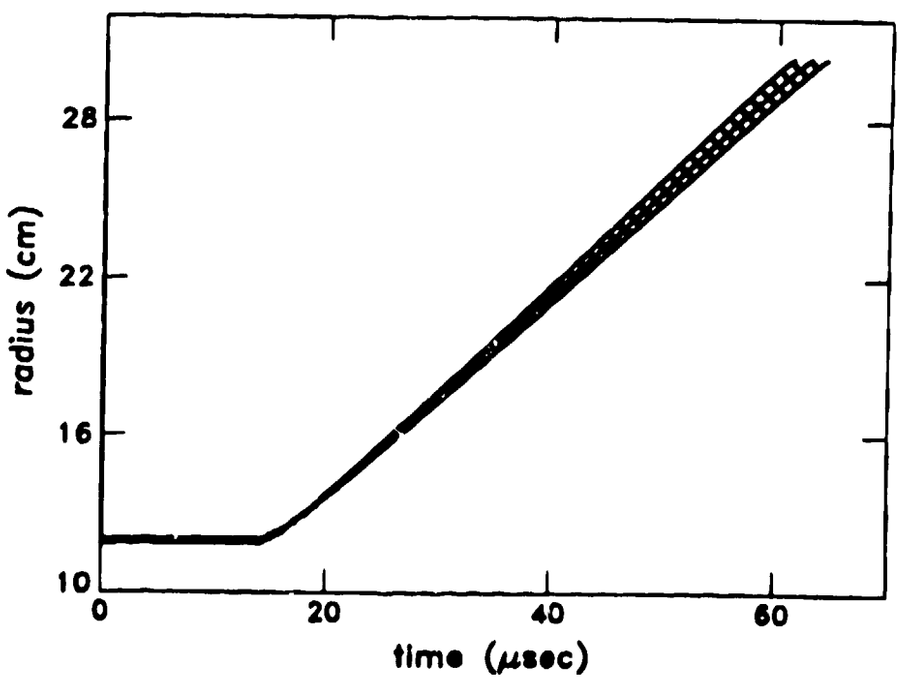

Fig. 7. Armature interface position at 7, 21, 35, 49, and 63 cm from the feed end glide plane. The different curves show the effect of the armature shim.

was empirically chosen to match results of 1-D and 2-D MHD calculations for similar but simpler geometries. Results of the circuit simulation predictions are presented in Fig. 8 below with the measured performance of the FCG. Discrepancies are discussed following the experimental results.

IV. EXPERIMENTAL RESULTS

The initial seed current was measured as 2.93 ± 0.09 MA by a Rogowsky loop at the feed end of the FCG. Crowbar of the capacitor bank occurred 2 μs before first armature motion, as planned. The final current at generator burnout appears to be 72.4 ± 3.6 MA, ~38% below expected performance. Ar experimental current trace, averaged over 5 $\dot{B}$ probes plus data from a fiber optic diagnostic[8] are presented in Fig. 8 with results of the circuit modeling. The theoretical uncertainty envelope (dashed line) was obtained by arbitrarily applying a 10% uncertainty to $\phi(t_{burnout})/\phi_0$ and using the experimental uncertainty associated with the seed current. Several of the probes gave erratic signals just at expected burnout time, then continued to indicate further compression. However, after burnout time, data from different probes are not quantitatively consistent; one probe even indicated a negative dI/dt. Only reliable and consistent data are presented in Fig. 8.

V. DISCUSSION

Gain

The FCG did not perform as well as predicted with respect to overall gain. The actual gain was only 24.7 compared to a predicted gain of ~38. The candidate which may be responsible for the largest discrepancy is the physical state of the armature near the glide planes. The armature, quite thin by usual standards, is slammed into the 10° canted brass glide planes as well as being stretched and thinned near the ends. If the combination of elastic-plastic flow heating, compressional heating, and Joule heating of the thinned armature caused it to melt (or come close), its resistivity and thus magnetic flux-loss would increase dramatically. This possibility was not incorporated into the theoretical modeling. Quantitative treatment of this flux-loss mechanism requires a detailed 2-D MHD calculation using accurate equations of state, and accurate models for material strength and electrical resistivity.

Another possible discrepancy lies in the electrical resistivity model. However, since the models used in these calculations have been benchmarked in other experiments,[9] it is unlikely that the model itself could account for the entire discrepancy.

Finally, a shock traveling through the load end glide plane could have interferred with the diagnostics several microseconds before burnout. This would imply that the air gap included below the load ring to diffuse any shocks was ineffective, and that the predicted generator run time was off by ~4 μs. Assuming that both of these are true, the FCG could have generated in excess of 72 MA, after the diagnostics became unreliable. Based on calculations and experience with HE, as well as the fact that all current traces seemed to level off before becoming erratic, this seems to be the least likely scenario.

Shape

The shape of the current profile in Fig. 8 is somewhat puzzling. During the early portion of generation, the FCG actually performed significantly better than predicted. In Fig. 9, the same experimental data are compared to circuit simulations

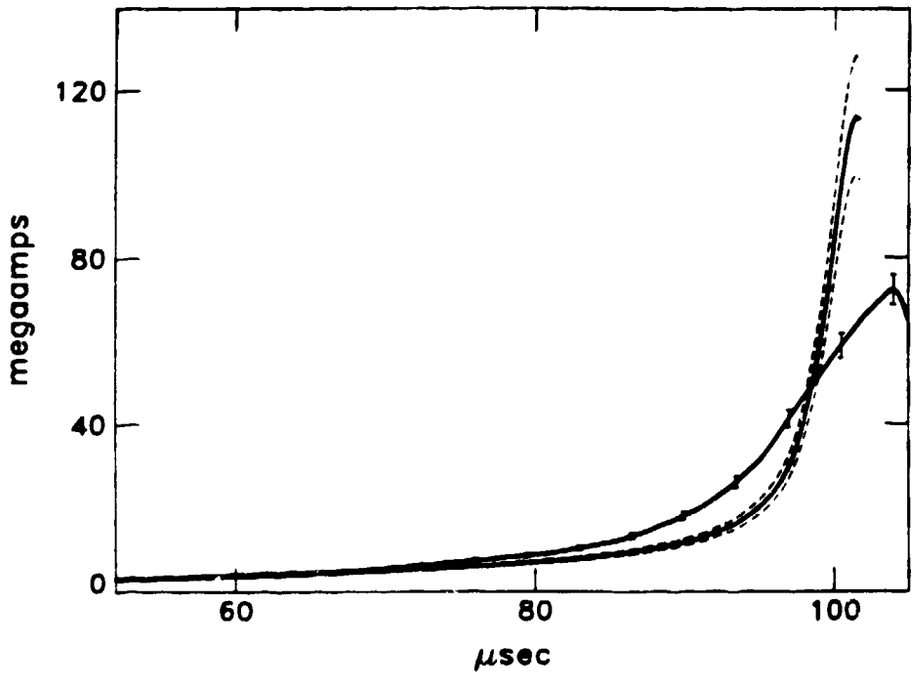

Fig. 8. Comparison of experimental current trace (with error bars) and circuit model prediction (solid and dashed) using $\phi = \phi_0 \exp[-(t/\tau)^2]$.

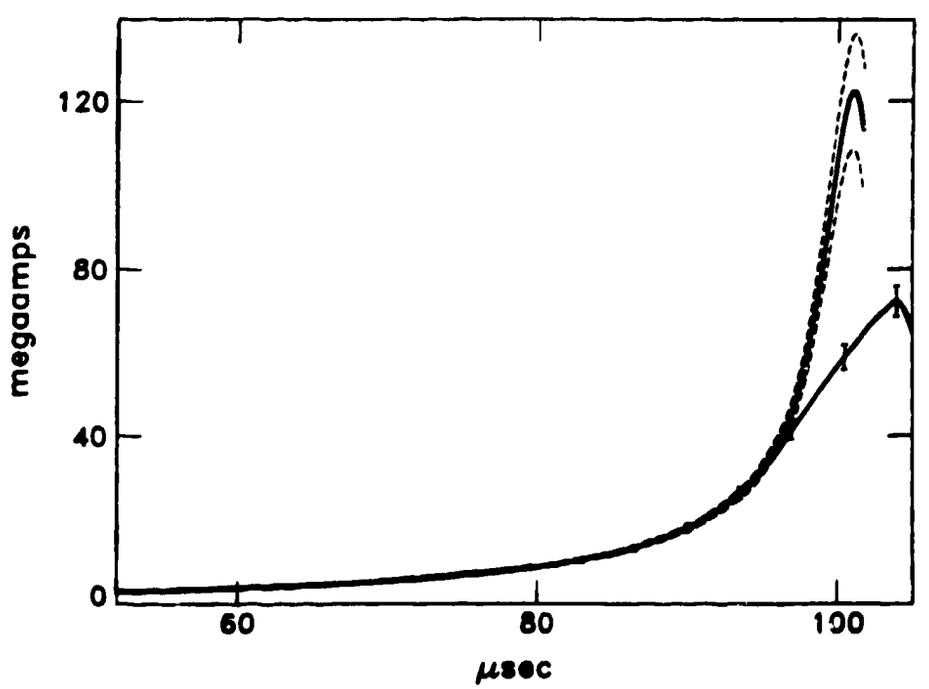

Fig. 9. Comparison of experimental current trace (with error bars) and circuit model prediction using $\phi = \phi_0 \exp[-(t/\tau)^{12}]$.

using $\phi(t) = \phi_0 \exp(-(t/\tau)^{12})$. This flux-loss model forces the FCG to perform lossless during most of its generation time and then lose flux rapidly just before burnout. Assuming that the data are correct, the FCG appeared to perform very efficiently until the last 10 μs of its 52 μs generation time, indicating that the shock-absorbing layer worked very well. At late times, the armature may have thinned sufficiently to activate nonlinear diffusion processes. This would account for the good efficiency at early times as well as the disappointing gain.

The timing difference in Figs. 8 and 9 between prediction and experiment is easily accounted for by uncertainties in the equations of state, particularly the one for polystyrene, and experimental timing uncertainties.

Summary

In summary, this FCG has been tested only once and has not had the benefit of empirical design optimization. The design was guided by theory and worked reasonably well on the first shot. Further analysis and possible experiments will help with understanding the discrepancy between the theoretical and experimental gain.

IV. REFERENCES

1. H. Knoepfel, Pulsed High Magnetic Fields, (North Holland Pub. Co.) pg. 10-13, (1970).
2. Y. P. Terletskii, Zh. Eskp. Teor. Fix 32, 387 (1957) [Sov. Phys. JETP 5, 301 (1975)].
3. C. M. Fowler, W. B. Garn, and R. S. Caird, J. Appl. Phys. 31, 588 (1960).
4. A. D. Sakharov, R. Z. Lyudaev, E. N. Smirnov, Yu. I. Plyushchev, A. I. Pavlovskii, V. K. Chernyshev, E. A. Feoktistova, E. I. Zharinov, and Yu. A. Zysin, Dokl. Akad. Nauk 165, 65 (1965) [Sov. Phys. Dokl., 10, 1045 (1966)].
5. A. D. Sakharov, Usp. Fiz. Nauk 88 725 (1966) [Sov. Phys. Usp. 9, 294 (1966)].
6. J. W. Shearer, F. F. Abraham, C. M. Alpin, B. P. Benham, J. E. Faulkner, F. C. Ford, M. M. Hill, C. A. McDonald, W. H. Stephens, D. J. Steinberg, and J. R. Wilson, J. Appl. Phys. 39, 2102 (1968).
7. Ye. I. Zharinov, V. A. Denidor, A. I. Ryabikin, and V. K. Chernyshev in Ultrahigh Magnetic Fields Physics Techniques Applications, pg. 298, Moscow Nauka (1984), Ed. V. M. Titov and G. A. Shvetsov.
8. L. R. Veeser, R. S. Caird, B. L. Freeman, D. R. Kania, P. J. Kruse, R. J. Trainor, and E. L. Zimmermann, in Proc. of 4th IEEE Pulsed Power Conference, p. 289, Albuquerque, NM (1983). ed. T. H. Martin and M. F. Rose.
9. I. R. Lindemuth, J. H. Brownell, A. E. Greene, G. H. Nickel, T. A. Oliphant, and D. L. Weiss, J. Appl. Phys., 57, 4447 (1985).